Tailoring the Surface Architecture of Poly(3-hydroxybutyrate-*co*-4-hydroxybutyrate) Scaffolds

S. Vigneswari,[1] M. I. A. Majid,[2] A. A. Amirul[1,2]

[1]*School of Biological Sciences, Universiti Sains Malaysia, 11800 Penang, Malaysia*
[2]*Malaysian Institute of Pharmaceuticals and Nutraceuticals, MOSTI, Malaysia*

Received 6 June 2011; accepted 13 July 2011
DOI 10.1002/app.35336
Published online 3 November 2011 in Wiley Online Library (wileyonlinelibrary.com).

ABSTRACT: This study was designed to determine whether the surface modifications of the various poly(3-hydroxybutyrate-*co*-4-hydroxybutyrate) [P(3HB-*co*-4HB)] copolymer scaffolds fabricated would enhance mouse fibroblast cells (L929) attachment and proliferation. The P(3HB-*co*-4HB) copolymer with a wide range of 4HB monomer composition (16–91 mol %) was synthesized by a local isolate *Cupriavidus* sp. USMAA1020 by employing the modified two-stage cultivation and by varying the concentrations of 4HB precursors, namely γ-butyrolactone and 1,4-butanediol. Five different processing techniques were used in fabricating the P(3HB-*co*-4HB) copolymer scaffolds such as solvent casting, salt-leaching, enzyme degradation, combining salt-leaching with enzyme degradation, and electrospinning. The increase in 4HB composition lowered melting temperatures (T_m) but increased elongation to break. P(3HB-*co*-91 mol % 4HB) exhibited a melting point of 46°C and elongation to break of 380%. The atomic force analysis showed an increase in the average surface roughness as the 4HB monomer composition increased. The mouse fibroblasts (L929) cell attachment was found to increase with high 4HB monomer composition in copolymer scaffolds. These results illustrate the importance of a detailed characterization of surface architecture of scaffolds to provoke specific cellular responses. © 2011 Wiley Periodicals, Inc. J Appl Polym Sci 124: 2777–2788, 2012

Key words: biosynthesis; poly(3-hydroxybutyrate-*co*-4-hydroxybutyrate); cytocompatibility; scaffolds; proliferation

INTRODUCTION

Scaffolds used in tissue engineering applications should ideally mimic the structural and functional profile of the materials found in the native extracellular matrix. The architecture of the scaffolds plays a crucial role on its efficiency and should be chosen or tailored in accordance to the requirements in the respective anatomical locations.[1] To date, different fabrication techniques had resulted in scaffolds with distinctive architecture. Various types of polymers, both synthetic and natural have been used to fabricate scaffolds for selected medical applications and they have shown good biocompatibility. Over the past decade, research on scaffolds made from biodegradable polymers has resulted in significant findings addressing its physical and mechanical properties, architecture, and efficacy of cell–biomaterial interactions.[2] These polymers can be tailored according to its specificity for various tissue engineering applications.[3] Nevertheless, no single existing polymeric scaffold can suffice for all the medical applications.

Polyhydroxyalkanoate (PHA), a well known class of biodegradable polymer has gained much attention as a promising biomaterial. Poly(3-hydroxybutyrate-*co*-4-hydroxybutyrate) [P(3HB-*co*-4HB)] copolymer, in particular, exhibits good biocompatibility, resorbability, and elastomeric properties.[4] Hydrolysis of P(3HB-*co*-4HB) yields 4-hydroxybutyrate (4HB), which is a natural human metabolite present in the brain, heart, lung, liver, kidney, and muscle.[5] P(3HB-*co*-4HB) is easily processable, sterilizable, and capable of controlled stability or degradation in response to biological conditions.[6] It is one of the most sought after PHA-based biomaterial for medical applications.[7] A wide variety of P(3HB-*co*-4HB) copolymer with interesting physical properties which favors specific medical applications can be achieved by varying the 4HB content.[8,9] By fusing suitable processing techniques with P(3HB-*co*-4HB) copolymer of desired characteristics, scaffolds with good physical property and surface architecture can be fabricated.

In this study, efforts were taken to achieve the above. By using a locally isolated *Cupriavidus* sp. USMAA1020, P(3HB-*co*-4HB) copolymer with precisely regulated 4HB molar fraction were produced using a modified two-stage cultivation technique. These copolymers were then used to fabricate

Correspondence to: A. A. Amirul (amirul@usm.my).
Contract grant sponsor: USM Fellowship.

scaffolds by employing different techniques to attain scaffolds with various characteristics and surface morphology. The biocompatibility of P(3HB-*co*-4HB) copolymer scaffolds were evaluated by L929 cell interaction and proliferation parallel to their architectural parameters. The results obtained showed that P(3HB-*co*-4HB) copolymer with high fractions of 4HB could be produced using the modified cultivation method. The fabrication technique detailed herein allows for development of scaffolds with porous architecture which has high potentials of being developed as medical implants. In addition, the scaffold fabrication techniques adopted in this study are versatile and has general applicability to other polymers.

EXPERIMENTAL

Biosynthesis of P(3HB-*co*-4HB) copolymer using modified two-stage cultivation

Biosynthesis of P(3HB-*co*-4HB) was carried out using two-stage cultivation technique as described by Amirul et al. with some modification.[10] In this modified two-stage cultivation, a total of 8 L of culture medium was used in a 10-L (B.Braun-Biostat D, Germany) fermenter. Initially, 4 L of nutrient rich (NR) medium was inoculated with *Cupriavidus* sp. USMAA1020 seed culture (10% v/v) and grown in the fermenter for 8–10 h (1.0 g/L). Later, 4 L of mineral medium (MM) was added into the fermenter, making the total working volume 8 L. Carbon source, trace elements (1.0 mL), and 0.1*M* $MgSO_4.7H_2O$ (10 mL) were added at this time. The culture was later agitated at 350 rpm for 48 h at room temperature. Type and concentrations of carbon source used were varied to obtain copolymers with desired 4HB content. Sampling was done at intervals of every 12 h. On the other hand, copolymer with 91 mol % 4HB was produced by degrading P(3HB-*co*-70%4HB) [obtained from the Institute of Pharmaceutical and Nutraceutical Malaysia] with depolymerase enzyme from *Acidovorax* sp. (DP5).

Solvent cast scaffolds

PHA was extracted by stirring freeze-dried cells in chloroform (1 : 200 w/v) for 24 h at room temperature. The concentrated solution was then precipitated with chilled methanol and recovered by filtration using a 0.45 μm polytetrafluoroethylene (PTFE) membrane before leaving to air dry in a fume cupboard under room temperature. Solvent cast PHA films were obtained by dissolving 0.75 g of extracted polymer in 20 mL of chloroform and transferred into a glass Petri dish (diameter of 90 mm) which served as a casting surface. The petri dish was left overnight for evaporation of chloroform under room temperature. Complete evaporation resulted in the formation of PHA films which were used as solvent cast scaffolds. The films were aged for 1 week prior to analysis to reach equilibrium crystallinity.

Particle-leached scaffolds

Particle-leached scaffolds were prepared as described previously.[11] Extracted PHA was dissolved in chloroform 3.75% (w/v). Then pre-sieved NaCl particles (100–200 μm) were added into the polymer solution. Salt to polymer ratio was maintained at 95 : 5. The vortexed dispersion was cast into a glass Petri dish. After air drying in a fume cupboard for 48 h at room temperature, the resulting polymer/salt composite was immersed in distilled water to leach out the salt which then resulted in sponge-like scaffolds. The scaffolds were then air dried for 24 h and later vacuum dried for another 48 h in a fume cupboard at room temperature to remove remaining solvent.

Enzyme eroded scaffolds

Enzyme eroded scaffolds were prepared as described previously.[12] Solution cast PHA film was first cut into pieces of 10 mm × 10 mm in size. These pieces of films were then immersed in 40 mL glycine-NaOH buffer solution containing 0.05 unit of depolymerase enzyme from *Acidovorax* sp. (DP5) in a 250-mL conical flask. The reaction mixture was incubated at 37°C in an incubator shaker at 180 rpm. After 10–12 h (above this time, the polymer gradually disappears) of incubation, the films were removed and rinsed with water and dried to constant weight.

Particle-leached and enzyme eroded scaffolds

The particle leached scaffolds were prepared as described above. Subsequently, the pieces of scaffolds (10 mm × 10 mm in size) were eroded using depolymerase enzyme as described above but only incubated for a period of 2 h.

Electrospun scaffolds

Electrospinning of PHA was performed using Esprayer ES-2000 (Fuence, Co. Ltd., Japan) instrument as described by Ying et al. but with some modification.[13] Polymer solution of 3% w/v was prepared by dissolving 0.3 g of PHA in 10 mL mixed solvent of dimethylformamide (DMF) and chloroform (v/v) prepared at a ratio of 1 : 4. The polymer solution was placed in a 1 mL glass syringe which was set vertically. The solution was extruded at a constant rate of 40 μL/min. A positive voltage of

20 kV was applied. Electrospinning was carried out at room temperature with a chamber humidity of 32–35%. The electrospun fibers were collected on a circular collecting area which was created using a nonconductive plastic layered with a sheet of aluminum foil and placed on the copper plate.

Gas chromatography analysis

To determine the monomer composition and intracellular PHA content, gas chromatography (GC) analysis was carried out. Approximately 10–15 mg of the freeze-dried cells or extracted polymer were subjected to methanolysis in the presence of methanol and sulfuric acid [85% : 15% (v/v)] at 100°C for 3 h to convert monomer units to their corresponding methyl esters. The resulting methyl esters were analyzed by GC (GC 2014, Shimadzu, Japan).[14]

Gas permeation chromatography analysis

The molecular weight of PHA was analyzed using a Waters 600E gas permeation chromatography (GPC) system and Waters 410 refractive index detector with a PLgel Mixed C column (Polymer Laboratories, Ltd., UK). Chloroform was used as the eluent at a flow rate of 0.8 mL/min. The sample concentrations and injection volumes were 0.1% (w/v) and 20 μL, respectively. Polystyrene standards with a low polydispersity were used to construct a calibration curve.[10,15,16]

Thermal properties

Thermal characterization was carried out using a differential scanning calorimeter (DSC) [Pyris 1 DSC, Perkin–Elmer]. PHA samples (8–10 mg) were encapsulated in aluminum pans and heated at a rate of 10 °C/min from −50 to 200°C (first heating run). After the first heating run, the sample was cooled to −50°C at a rate of 20 °C/min. Then, the sample was heated again at a rate of 10 °C/min to 200°C (second heating run). The melting temperature (T_m) was determined from the DSC endotherms. The glass transition temperature (T_g) was taken as the midpoint of the heating capacity change.[10,16]

Tensile property

Tensile test was carried out using tensile testing machine (GoTech A1-3000, Taiwan) at a cross-head speed of 10 mm/min under room temperature. The films were aged for 1 week prior to analysis to reach equilibrium crystallinity. Tensile test pieces were cut into dumbbell shapes using steel ASTM regulation punches (4 mm width, 75 mm gauge length) from solvent cast PHA films. The thickness of each test piece was measured before testing. Tensile data were calculated from the stress–strain curves of an average of three specimens.

Atomic force microscopy

The surface roughness of the solvent cast scaffolds were analyzed using atomic force microscopy (AFM) [S110, Japan]. The resonance frequency was set at 300 kHz. Meanwhile, the sampling areas were standardized at 5 μm × 5 μm. Five different spots per film were analyzed.[17,18]

Water uptake ability

The PHA films and scaffolds were dried in an oven until there were no changes in weight loss. The specimens were then immersed in distilled water containing 0.05% (w/v) sodium azide at 37°C for a period of 8 weeks. The dry weight before immersion (m_o) and wet weight (m_f) after immersion were recorded. Water uptake was calculated using the formula below[19]:

$$\text{Water uptake} = (m_f - m_o)/m_o \times 100\%$$

Pore size and porosity calculation

Porosity of the scaffolds was calculated using Image Analyzer Software. Values of 100 different spots were analyzed and averaged.[20]

Scanning electron microscopy

The surface morphology of PHA films and scaffolds were also observed using Scanning electron microscopy (SEM) (Leo Supra 50 VP Field Mission SEM, Carl-Ziess SMT, Germany). Samples were mounted on aluminum stumps coated with gold in a sputtering device before viewing under the SEM.

In vitro cytotoxicity evaluation

The L929 cell line was cultured in MEM (Modified Eagle Medium) supplemented with 2 m*M* L-glutamine, 10% fetal calf serum, and 1% penicillin-streptomycin solution. Culture was grown in polystyrene flasks and incubated in a 5% CO_2 incubator at 37°C. Culture medium was changed at 2 days intervals.

P(3HB) and P(3HB-*co*-4HB) scaffolds as well as the positive control poly(L-lactic acid) (PLLA) film (6 mm in diameter) were then seeded with L929 cells (1.0×10^4 cells/mL) for 96 h. The scaffolds and PLLA film were previously sterilized under UV crosslinker (Spectrolinker, XL-1000 UV Crosslinker, New York) at 1200 μJ/cm^2 for 30 min.

TABLE I
Synthesis of P(3HB-*co*-4HB) Copolymer by *Cupriavidus* sp. USMAA1020 Using Modified Two-Stage Cultivation Process[a]

Carbon content (wt %)		Dry cell weight (g/L)	PHA content (wt %)	PHA composition (mol %)		PHA concentration (g/L)[b]
1,4-Butanediol	γ-Butyrolactone			3HB	4HB	
–	–	10.34 ± 0.16	33.9 ± 1.3	100	0	3.50 ± 0.22
–	0.56	7.82 ± 0.11	32.3 ± 1.6	85	16	2.52 ± 0.25
–	0.85	8.55 ± 0.06	23.4 ± 1.1	71	29	2.00 ± 0.21
0.75	0.20	7.40 ± 0.05	16.4 ± 1.4	55	45	1.57 ± 0.08
–	0.56[c]	9.51 ± 0.06	12.3 ± 0.9	37	63	1.17 ± 0.09

[a] The cells were harvested after 48 h of incubation in a 10-L bioreactor at 350 rpm, 1 vvm at 28°C with an initial pH of 7.0.
[b] PHA concentration = PHA content × dry cell weight.
[c] γ-butyrolactone of 0.28 (carbon wt %) was sequentially fed at intervals of 12 h (12 h-0.28 + 24 h-0.28).
Cells were cultured in nutrient rich medium containing 0.56% carbon (wt %) oleic acid in the first stage of production (growth phase).

The cell viability and proliferation was assayed with MTS [3-(4,5-dimethylthiazol-2-yl)-5-(3-carboxymethoxyphenyl)-2-(4-sulfophenyl)-2*H*-*t*etrazolium] and PMS [phenazine methosulfate] (CellTiter 96® Aqueous Non-Radioactive Cell Proliferation Assay, Promega) as described previously (Chee et al., 2008; Vigneswari et al., 2009). Briefly, a total of 20 μL of the combined MTS/PMS solution was pipetted into each well containing the cells seeded onto the scaffolds and was incubated for another 1–4 h in the 5% CO_2 incubator at 37°C incubator. The absorbance of formazon produced was measured using a Microplate Reader (Bio-Rad 680, UK) at 490 nm. A standard curve of absorbency values plotted against cell count was established as previously described.[16,21] Viable number of cells on polymer scaffolds was then determined from this standard curve based on their MTS absorbency. Experiments were carried out in replicates of four.[21]

RESULTS

Biosynthesis and characterization of P(3HB-*co*-4HB) copolymer

Cupriavidus sp. USMAA1020 was able to produce P(3HB-*co*-4HB) copolymer with different 4HB monomer composition when precursor carbon and its concentration was varied (Table I). P(3HB-*co*-16 mol % 4HB) and P(3HB-*co*-29 mol % 4HB) were produced by single feeding of γ-butyrolactone, whereas, copolymer with 63 mol % 4HB was obtained by sequential feeding. On the other hand, copolymer with a high 4HB molar fraction of 45 mol % was produced by feeding a combination of 1,4-butanediol and γ-butyrolactone. Nevertheless, for the production of P(3HB), oleic acid was fed as sole carbon source.

The molecular weights, thermal, and mechanical properties of the various P(3HB-*co*-4HB) copolymers are listed in Table II. The M_n of copolymers decreased from 216 ± 10 to 68 ± 4 kDa with increasing 4HB molar fraction (16–91 mol %). Meanwhile, polydispersity ranged from 1.5 ± 0.3 to 2.1 ± 0.2. On the other hand, the T_m was also found to decrease with higher 4HB monomer fraction. P(3HB) exhibited a high T_m of (167 ± 1)°C, whereas, the value decreased to as low as (46 ± 3)°C when 91 mol % of 4HB was present. A drastic decrease in T_m value of about 90°C was observed between copolymers containing 63 mol % and 91 mol % of 4HB. The tensile strength and elongation to break of P(3HB-*co*-4HB) copolymers ranged from 5 ± 1 to 9 ± 2 MPa and 80 ± 11 to 380 ± 53%, respectively.

TABLE II
The Molecular Weights, Thermal, and Mechanical Properties of P(3HB-*co*-4HB) Copolymer Synthesized Using Modified Two-Stage

Polymer	M_n[a] × 10^3 (Da)	M_w/M_n[a]	Glass transition temperature[b] (°C) (T_g)	Melting temperature[b] (°C) (T_m)	Tensile strength (MPa)[c]	Elongation to break (%)[c]
P(3HB)	250 ± 7	1.3 ± 0.40	1 ± 0	167 ± 1	4 ± 2	6 ± 1
P(3HB-*co*-16%4HB)	216 ± 10	1.5 ± 0.30	−11 ± 1	164 ± 2	7 ± 1	234 ± 14
P(3HB-*co*-29%4HB)	152 ± 11	1.7 ± 0.30	−12 ± 1	161 ± 2	5 ± 3	80 ± 11
P(3HB-*co*-45%4HB)	130 ± 8	2.1 ± 0.20	−15 ± 1	160 ± 1	5 ± 1	190 ± 17
P(3HB-*co*-63%4HB)	114 ± 9	1.9 ± 0.10	−11 ± 0	137 ± 2	6 ± 1	220 ± 10
P(3HB-*co*-91%4HB)	68 ± 4	1.8 ± 0.20	−22 ± 2	46 ± 3	9 ± 2	380 ± 53

[a] Calculated from GPC analysis; M_n: number-average molecular weight; M_w/M_n : polydispersity index.
[b] Calculated from DSC analysis.
[c] Determined using GoTech A1-3000 Tensile Machine.

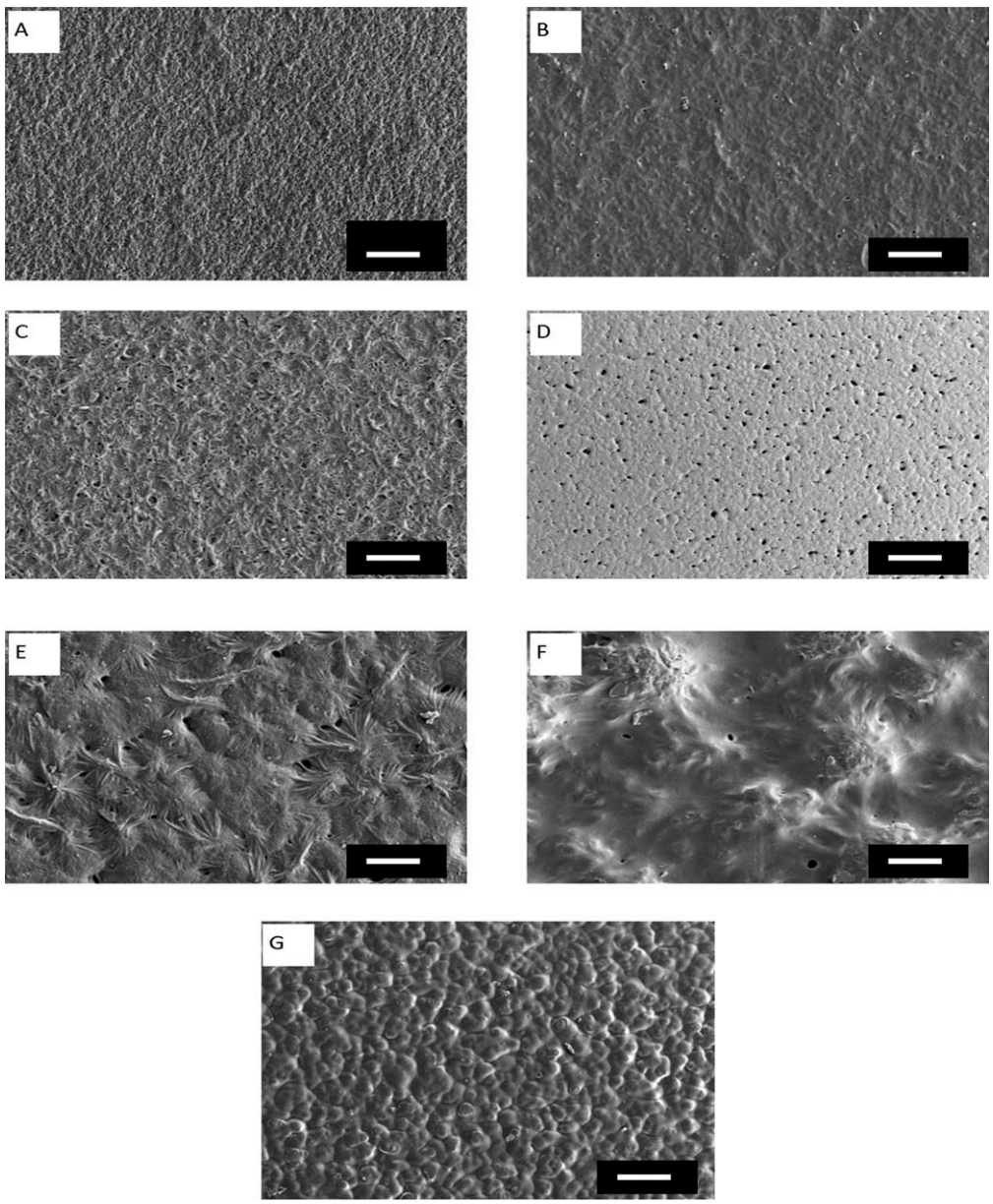

Figure 1 SEM micrographs of various P(3HB-*co*-4HB) solvent cast scaffolds. (A) P(3HB); (B) P(3HB-*co*-16%4HB); (C) P(3HB-*co*-29%4HB); (D) P(3HB-*co*-45%4HB); (E) P(3HB-*co*-63%4HB); (F) P(3HB-*co*-91%4HB); and (G) PLLA.

Surface morphology of different types of P(3HB *co*-4HB) scaffolds

The P(3HB-*co*-4HB) scaffolds were observed under SEM to determine their surface morphology. The surface morphology of scaffolds varied according to different processing techniques. In general, solvent cast scaffolds with higher 4HB monomer composition exhibited a rougher surface (Fig. 1). A more porous surface was observed with salt-leached and enzyme degraded scaffolds. Salt-leached scaffolds exhibited macroporous cavity formed by the leached NaCl particles within the polymer matrix (Fig. 2). Meanwhile, enzyme degraded scaffolds had a rough appearance and possessed numerous pits of varying size (Fig. 3). The surface of scaffolds fabricated using both salt-leaching and enzyme degradation technique possessed deep cavities and large pores (Fig. 4). On the other hand, electrospun P(3HB-*co*-4HB) copolymer scaffolds displayed a surface with layers of overlapping nanofibers (Fig. 5). It was observed that the fibers were more evenly distributed in copolymers with higher 4HB monomer composition.

Surface topography and roughness of P(3HB-*co*-4HB) cast films

AFM was used to analyze surface roughness of P(3HB-*co*-4HB) copolymer cast films. The AFM images showed that P(3HB-*co*-91%4HB) film had a rougher surface containing more uniform and larger

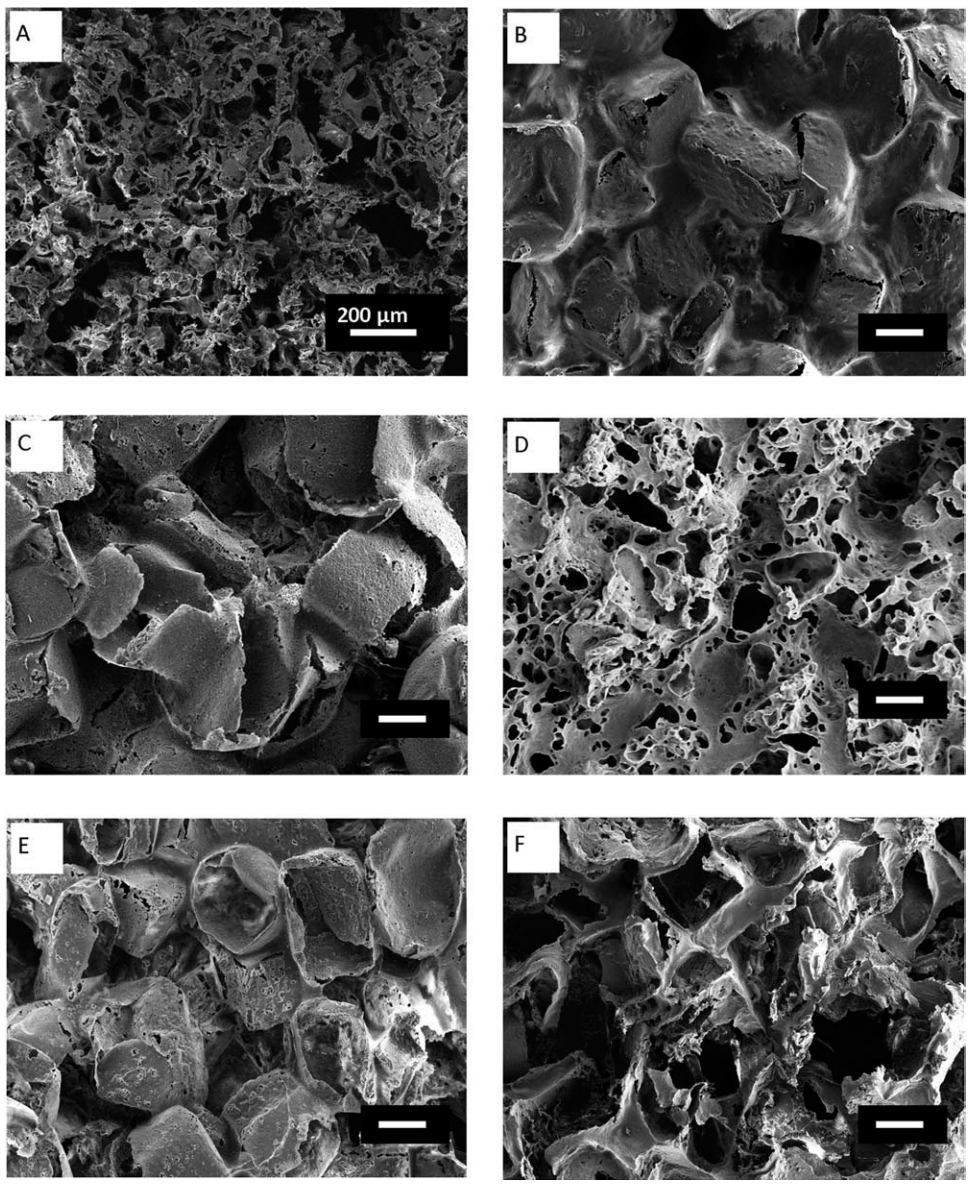

Figure 2 SEM micrographs of various P(3HB-*co*-4HB) copolymer scaffolds fabricated by salt-leaching technique. (A) P(3HB); (B) P(3HB-*co*-16%4HB); (C) P(3HB-*co*-29%4HB); (D) P(3HB-*co*-45%4HB); (E) P(3HB-*co*-63%4HB); and (F) P(3HB-*co*-91%4HB).

protuberances as compared to the other films. On the other hand, P(3HB-*co*-45%4HB) and P(3HB-*co*-63%4HB) films could also be decorated with a relatively high porosity. Pores could be observed in each 5×5 μm^2 area examined. In contrast, P(3HB), P(3HB-*co*-16%4HB), and P(3HB-*co*-29%4HB) films had a smoother surface, containing only a few smaller protuberances (Fig. 6). The average surface roughness among solvent cast scaffolds revealed an increase with higher 4HB monomer composition (Table III).

Pore size analysis

Based on the results obtained (Table IV), porosity of salt-leached scaffolds was found to increase (112.8 ± 5.8 to 218.0 ± 6.7 μm) with increasing 4HB monomer composition. Meanwhile, scaffolds prepared from the combination of salt-leaching and enzyme degradation technique exhibited smaller pore sizes in the range of 30.1 ± 2.1 to 59.1 ± 3.8 μm except for the scaffold with 91 mol % 4HB which recorded average pore sizes of 209.8 ± 9.7 μm. The pore size of salt leached scaffold with 91 mol % 4HB was the largest at 209.8 μm. Electrospun scaffolds of P(3HB-*co*-4HB) copolymers exhibited much smaller pore sizes in the range of 1.4 ± 0.2 to 2.3 ± 0.3 μm, which were almost similar to the pore sizes of P(3HB) electrospun scaffold. This could be due to the multiple overlays of nanofibers which restricts the pore size. On the other hand, the enzyme degraded scaffolds

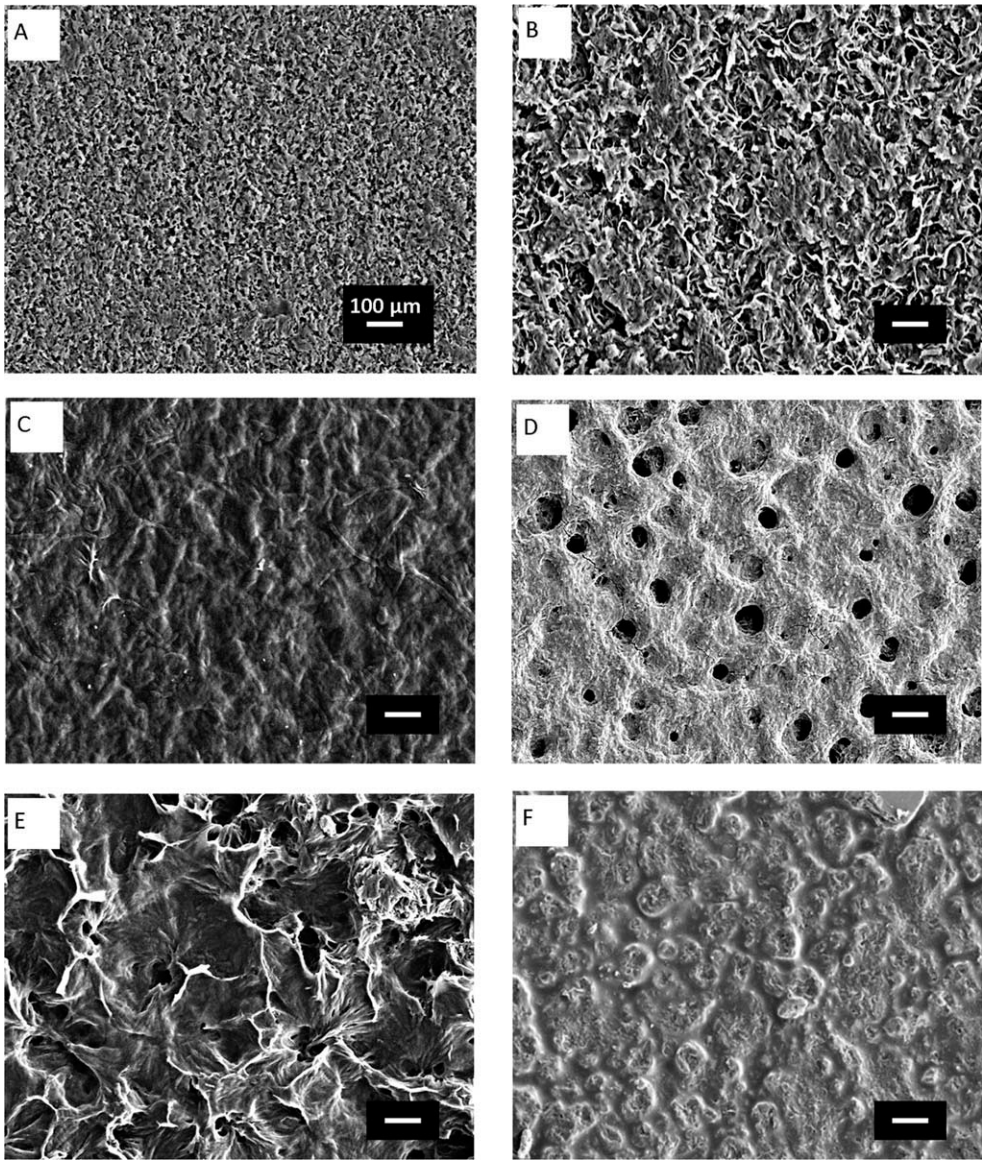

Figure 3 SEM micrographs of various P(3HB-*co*-4HB) copolymer scaffolds fabricated by enzyme degradation technique. (A) P(3HB); (B) P(3HB-*co*-16%4HB); (C) P(3HB-*co*-29%4HB); (D) P(3HB-*co*-45%4HB); (E) P(3HB-*co*-63%4HB); and (F) P(3HB-*co*-91%4HB).

exhibited smallest pore sizes ranging from 0.34 ± 0.03 to 0.60 ± 0.07 μm.

Water uptake ability

The water uptake ability of the various P(3HB-*co*-4HB) copolymer scaffolds is shown in Figure 7. It is observed that the percentage of water uptake of all copolymer scaffolds except electrospun scaffold increased in tandem with increasing 4HB monomer composition. Scaffolds prepared using P(3HB) showed values of less than 0.6%. Salt-leached scaffolds and scaffold prepared by the combined technique of salt-leaching and enzyme degradation exhibited higher water uptake ability compared to the others. Electrospun P(3HB-*co*-4HB) scaffolds were found to possess the least ability to retain water with values of less than 0.2%. Scaffold prepared from combination of salt-leaching and enzyme degradation using P(3HB-*co*-91%4HB) recorded the highest water uptake ability of 0.96% (w/w) after being saturated in aqueous solution.

Biocompatibility of P(3HB-*co*-4HB) scaffolds

Figure 8 shows the comparison of L929 cell growth on various P(3HB) and P(3HB-*co*-4HB) scaffolds. PLLA scaffold was used as a control and it exhibited cell viability of 2.9×10^5 cells/mL, the lowest number observed in this experiment. Based on the results, cell viability increased when scaffolds with higher 4HB monomer composition were used.

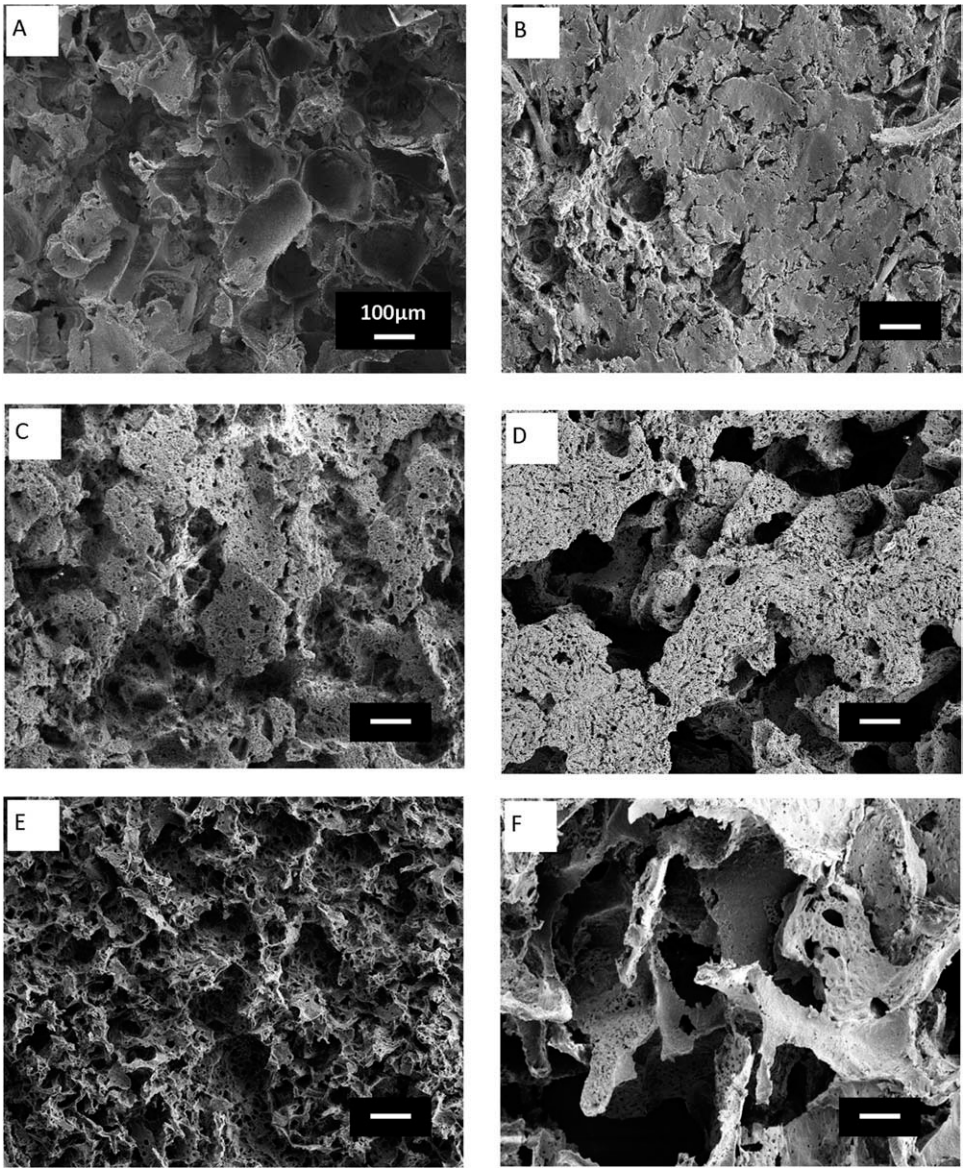

Figure 4 SEM micrographs of various P(3HB-*co*-4HB) copolymer scaffolds fabricated by combining salt-leaching and enzyme degradation technique. (A) P(3HB); (B) P(3HB-*co*-16%4HB); (C) P(3HB-*co*-29%4HB); (D) P(3HB-*co*-45%4HB); (E) P(3HB-*co*-63%4HB); and (F) P(3HB-*co*-91%4HB).

Scaffolds made using P(3HB-*co*-91%4HB) copolymer showed the highest cell viability which were approximately threefold (8.9×10^5 cells/mL) more than that of made using P(3HB). Generally, higher cell viability was recorded with the scaffold prepared by the combination of salt-leaching and enzyme degradation technique. The P(3HB-*co*-91%4HB) scaffold fabricated by this technique showed sevenfolds higher absorbance as compared to solvent cast film. On the other hand, similar type of scaffolds with 29, 45, and 63 mol % of 4HB showed significantly high cell viability as compared to other types of scaffold in their respective group. Proliferation of L929 cells on all P(3HB-*co*-4HB) scaffolds confirms that this copolymer does not exhibit cytotoxicity towards the cell.

DISCUSSION

Results obtained in previous studies have shown that one-stage cultivation does not seem to favor production of P(3HB-*co*-4HB) with high 4HB monomer composition as compared to two-stage cultivation when *Cupriavidus* sp. strains were used.[10,22] Amirul et al. observed 4HB accumulation of up to 51 mol % when two-stage cultivation was carried out in shake flask cultures using *Cupriavidus* sp. USMAA1020.[10] In this study, by employing a

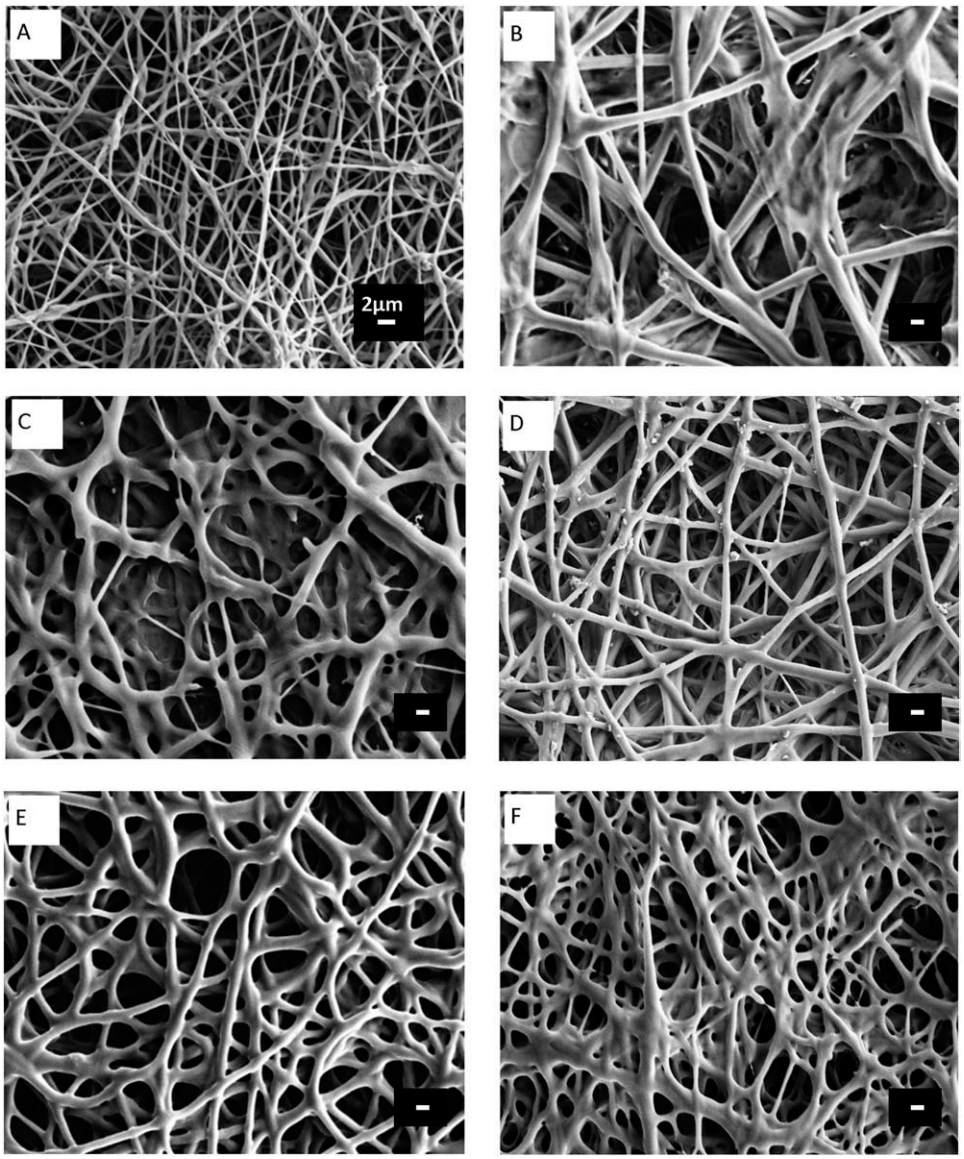

Figure 5 SEM micrographs of various P(3HB-*co*-4HB) copolymer scaffolds fabricated by electrospinning technique. (A) P(3HB); (B) P(3HB-*co*-16%4HB); (C) P(3HB-*co*-29%4HB); (D) P(3HB-*co*-45%4HB); (E) P(3HB-*co*-63%4HB); and (F) P(3HB-*co*-91%4HB).

modified two-stage cultivation method, P(3HB-*co*-4HB) copolymer with higher 4HB monomer composition (63 ± 2 mol %) was produced in fermenter scale experiment using the same strain. Addition of MM into NR containing *Cupriavidus* sp. USMAA1020 cells at their mid-exponential growth phase was found to promote increased cell biomass and copolymer accumulation (Table I). Feeding of a mixture of two carbon precursors (γ-butyrolactone and 1,4-butanediol) might have accelerated 4HB synthesis. Previously, similar finding reported a 4HB molar fraction of 84 mol % using similar combination of carbon sources via two-stage cultivation in shake flask cultures.[23]

Sequential feeding strategy is also known to result in improved production of copolymer and higher accumulation of secondary monomer.[24] By employing this modified two-stage cultivation for P(3HB-*co*-4HB) biosynthesis, the regular time consuming process of enrichment followed by aseptic transfer of bacterial cells into nitrogen-free MM containing carbon source could be resolved. A separation between the growth and production phase in the modified two-stage cultivation makes it possible to synthesize P(3HB-*co*-4HB) copolymer with tailored 4HB molar fractions. This form of separation cultivation strategy is convenient especially when employing two substrates for the synthesis of a copolymer.[25]

The M_n of a polymer is important in determining its strength as well as ability to be shaped and molded.[26] The M_n values of P(3HB-*co*-4HB) copolymers produced in this study falls in the range of 68–

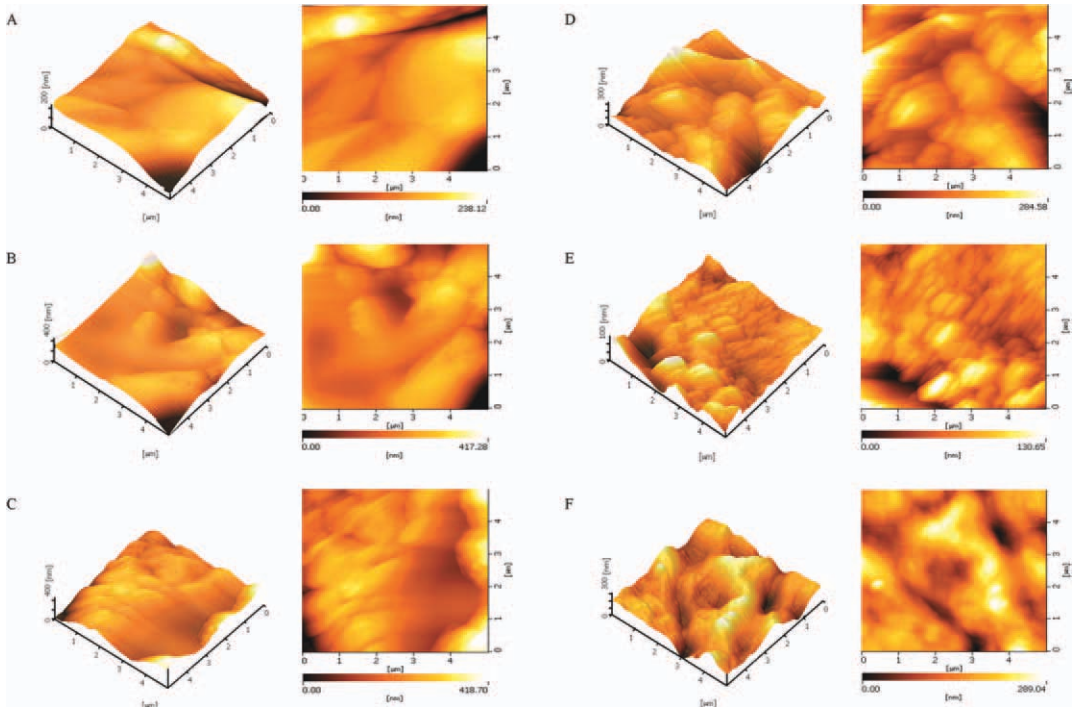

Figure 6 AFM images of surface topography of tested films. The surface roughness is represented by two-dimensional image (right) and three-dimensional image (left). (A) P(3HB); (B) P(3HB-*co*-16%4HB); (C) P(3HB-*co*-29%4HB) displays porous structure; (D) P(3HB-*co*-45%4HB); (E) P(3HB-*co*-63%4HB); and (F) P(3HB-*co*-91%4HB) displays dense porosity. Scan size 5.00 μm, scan rate 1 Hz. [Color figure can be viewed in the online issue, which is available at wileyonlinelibrary.com.]

250×10^3 Da (Table II). The M_n was found to decrease with increase in 4HB monomer composition. Similar observation was also reported in previous studies.[10,27,28] It was found that, the type and concentration of carbon sources supplied[29] and pH[30] of the culture medium are among the factors that influence the molecular weight of the PHA produced by a wide variety of bacteria.[8,31] Besides, different combination of carbon source and feeding strategy had also been reported to affect polymer M_n.[32–35] The feeding strategy adapted in this study which involves combination of carbon sources and sequential feeding at different intervals of cultivation might have influenced the M_n of the copolymer produced. Polydispersity index of P(3HB-*co*-4HB) produced in this study ranged from 1.3 to 2.1 (Table II). According to Riande et al., a polydispersity index close to 1 which is similar to that of polysterene is favored.[36] High polydispersity index means molecular weight distribution is relatively broad in the polymer.

Surface topography of the solvent cast copolymer scaffolds analyzed using AFM (Fig. 2) revealed that copolymer scaffolds with higher 4HB monomer composition had a rougher surface. P(3HB-*co*-91% 4HB) scaffold exhibited large protuberances. Notably, surface roughness greatly influences the interactions between cells and materials.[37]

The distribution of the uniformity and interconnection of the pores is fundamental in the fabrication of scaffolds as these features facilitate the penetration of fluids via the material and promote the formation of tissue in an organized network.[38] Cells that adhere to the surface of the scaffold absorb nutrients and remove metabolite through these pores.[39] This study demonstrated that salt-leached scaffold have higher porosity which increases with 4HB monomer composition (Table III). The P(3HB-*co*-4HB) copolymer was fused to form a continuous matrix with entrapped salt particles, and as the salt particles were leached, a macroporous surface was

TABLE III
Surface Roughness of Various P(3HB-*co*-4HB)[a]

Polymers	R_q (nm)	R_a (nm)
P(3HB)	1.35 ± 0.13	1.20 ± 0.33
P(3HB-*co*-16%4HB)	2.35 ± 0.21	1.66 ± 0.28
P(3HB-*co*-29%4HB)	4.93 ± 0.23	4.16 ± 0.11
P(3HB-*co*-45%4HB)	6.62 ± 0.11	5.34 ± 0.13
P(3HB-*co*-63%4HB)	9.08 ± 0.24	8.97 ± 0.21
P(3HB-*co*-91%4HB)	15.34 ± 0.45	14.32 ± 0.17

[a] Calculated from AFM based on the standard formula integrated in the software.

R_q: root mean square roughness; R_a: average roughness.

TABLE IV
Pore Size of Various P(3HB-*co*-4HB) Scaffolds[a]

Polymer	Salt-leached scaffolds (μm)	Salt-leached and enzyme degraded scaffolds (μm)	Electrospun scaffolds (μm)	Solvent cast (μm)	Enzyme degraded scaffolds (μm)
P(3HB)	88.7 ± 4.7	78.6 ± 3.9	1.1 ± 0.1	N.D	N.D
P(3HB-*co*-16%4HB)	112.8 ± 5.8	33.0 ± 1.3	1.4 ± 0.2	N.D	0.34 ± 0.03
P(3HB-*co*-29%4HB)	176.2 ± 9.4	48.8 ± 3.0	2.1 ± 0.1	N.D	N.D
P(3HB-*co*-45%4HB)	185.7 ± 8.8	59.1 ± 3.8	1.6 ± 0.2	N.D	0.60 ± 0.07
P(3HB-*co*-63%4HB)	198.2 ± 9.4	30.1 ± 2.1	1.7 ± 0.1	N.D	0.45 ± 0.06
P(3HB-*co*-91%4HB)	218.0 ± 6.7	209.8 ± 9.7	2.3 ± 0.3	N.D	N.D

N.D, not determined as these scaffolds does not produce significant porous structure as observed in SEM micrographs.
[a] The pore size of scaffold was estimated from SEM images using Image Analyser Software and it is a mean value of 100 readings.

produced. The use of salt particles of a controlled size is important in producing pores larger than 40 μm.[40] Degradation of PHA by extracellular depolymerase enzyme have been well studied.[35,41] Abe et al. reported that enzymatic degradation accelerates the rate of degradation and further increased the porosity of P(3HB) films.[41] The enzyme degraded copolymer scaffolds produced in this study showed the occurrence of very small pores of less than 1 μm. This method of fabrication was found to be not suitable in generating a porous P(3HB-*co*-4HB) scaffold.

Therefore, in this study, the porous salt-leached scaffolds are degraded with depolymerase enzyme to further enhance its porosity (Fig. 6). However, the enzymatic degradation of salt leached films did not further increase its pore size (Table III). In this case, salt-leached scaffolds that exhibited cavity formed by leaching of salts collapsed when degraded with enzyme. This resulted in a rougher and uneven surface.

Figure 7 shows P(3HB-*co*-4HB) copolymer scaffolds fabricated via electrospinning. Although this technique can produce highly porous scaffolds with interconnected pores suitable for tissue regeneration, this method involves the use of toxic solvents such as hexafluoroisopropanol (HFIP) and DMF which can reduce the proliferation of cells.[42] This explains the lower proliferation on electrospun scaffolds as compared to scaffolds fabricated by employing the combination of salt-leach and enzyme degradation. On the other hand, the water uptake of these scaffolds changed regularly with their compositions and surface morphology (Fig. 1). The absorption of water leads to faster degradation and the pores provides the space necessary for tissue invasion.[1,43]

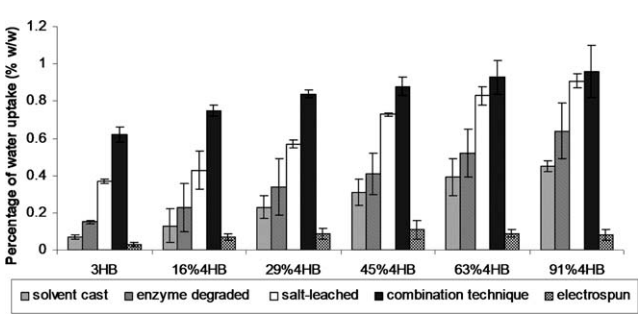

Figure 7 Water uptake ability of various P(3HB-*co*-4HB) scaffolds. Values are mean of three replicates.

Proliferation of cells on the PHA scaffolds increased in the order of P(3HB) < P(3HB-*co*-16% 4HB) < P(3HB-*co*-25% 4HB) < P(3HB-*co*-45% 4HB) < P(3HB-*co*-63% 4HB) < P(3HB-*co*-91% 4HB). This was further corroborated by the surface topography analyzed from AFM (Fig. 2). AFM revealed that P(3HB-*co*-91% 4HB) had a rougher surface with larger nano-sized protuberances. Notably, surface roughness greatly influences the interactions between cells and materials.[17,37] The surface topography and chemical constituent of a scaffold will determine whether biological molecules will be absorbed, thereby influencing the spreading, proliferating, and cellular differentiating.[44] Simply fabricating a highly porous scaffold and seeding it with the specific types of cells does not qualify a scaffold as the desired tissue-engineering material.[1] The tissue scaffold must be designed to satisfy several

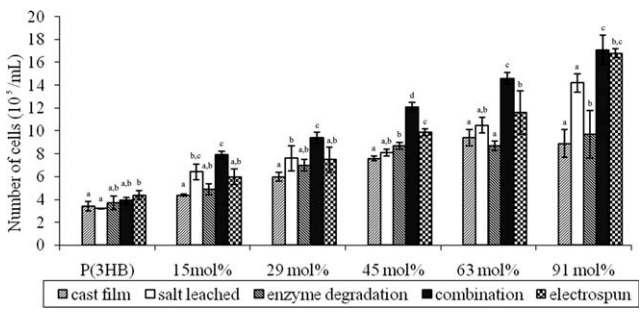

Figure 8 Proliferation of mouse fibroblasts (L929) cells cultured on various scaffolds of P(3HB), P(3HB-*co*-16%4HB), P(3HB-*co*-29%4HB), P(3HB-*co*-45%4HB), P(3HB-*co*-63%4HB), and P(3HB-*co*-91%4HB) after incubation for 4 days. Values are mean of four replicates. Mean data accompanied by different alphabets indicates significant difference within the group (Tukey's HSD test, $P < 0.05$).

requirements to mimic the properties of living systems.[2] However, no single technique can encompass all scales, in control of both architecture and surface chemistry.[1] This work has demonstrated that cells proliferate according to the surface morphology of the PHA polymer scaffolds.

CONCLUSIONS

The fabrication technique detailed herein allows the development of a wide range of architectural scaffolds parallel to the cell interaction. The findings of this study have generated some interesting subject matters which perhaps can be investigated in future works. The P(3HB-*co*-4HB) scaffolds produced in this study could be investigated as medical patches for controlled drug release or tissue regeneration *in vivo*. Composites of P(3HB-*co*-4HB) produced and other biomaterial can perhaps be developed and investigated for improved surface architecture.

Authors would like to thank MOSTI for the funding of this project and USM fellowship awarded to the author S.Vigneswari. Authors thank Assoc. Prof. Dr. Sudesh Kumar from Universiti Sains Malaysia for his assistance.

References

1. Mikos, A. G.; Herring, S. W.; Ochareon, P.; Elissenff, J.; Lu, H. H.; Kandel, R.; Schoen, F. J.; Toner, M.; Mooney, D. J.; Atala, A. Tissue Eng 2006, 12, 3307.
2. Liu, C.; Xia, Z.; Czernuszka, J. T. Chem Eng Res Des 2007, 85, 1051.
3. Matthews, J. A.; Wnek, G. E.; Simpson, D. G.; Bowlin, G. L. Biomacromolecules 2002, 3, 232.
4. Anderson, A. J.; Dawes, E. A. Microbiol Rev 1990, 4, 450.
5. Williams, S. F.; Martin, D. P. Biopolymers 2002, 3, 91.
6. Sudesh, K.; Gan, Z.; Maehara, A.; Doi, Y. Polym Degrad Stab 2002, 77, 77.
7. Martin, D. P.; Williams, S. F. Biochem Eng J 2003, 16, 97.
8. Saito, Y.; Nakamura, S.; Hiramitsu, M.; Doi, Y. Polym Int 1996, 39, 169.
9. Ishida, K.; Wang, Y.; Inoue, Y. Biomacromolecules 2001, 2, 1285.
10. Amirul, A. A.; Yahya, A. R. M.; Sudesh, K.; Azizan, M. N. M.; Majid, M. I. A. Bioresource Technol 2008, 99, 4903.
11. Suh, S. W.; Shin, J. Y.; Kim, J.; Beak, C. H.; Kim, D. I.; Kim, H.; Jeon, S. S.; Choo, I. W. ASAIO J 2002, 48, 460.
12. Saito, Y.; Doi, Y. Int J Biol Macromol 1994, 16, 99.
13. Ying, T. H.; Ishii, D.; Mahara, A.; Murakami, S.; Yamaoka, T.; Sudesh, K.; Samian, R.; Fujita, M.; Maeda, M.; Iwata, T. Biomaterials 2008, 29, 1307.
14. Braunegg, G.; Sonnleitner, B.; Lafferty, R. M. Eur J Appl Microbiol Biotechnol 1978, 6, 29.
15. Nishida, H.; Suzuki, S.; Konno, M.; Tokiwa, Y. Polym Degrad Stab 2000, 67, 291.
16. Vigneswari, S.; Vijaya, S.; Majid, M. I. A.; Sudesh, K.; Sipaut, C. S.; Azizan, M. N. M.; Amirul, A. A. J Ind Microbiol Biotechnol 2009, 36, 547.
17. Hu, Y. J.; Wei, X.; Zhao, W.; Liu, Y. S.; Chen, G. Q. Acta Biomater 2009, 5, 1115.
18. Ji, Y.; Li, X. T.; Chen, G.Q. Biomaterials 2008, 29, 3807.
19. Ying, T. H.; Ishii, D.; Mahara, A.; Murakami, S.; Yamaoka, T.; Sudesh, K.; Samian, R.; Fujita, M.; Maeda, M.; Iwata, T. Biomaterials 2008, 29, 1307.
20. Sun, J.; Wu, J.; Li, H.; Chang, J. Eur Polym Mater 2005, 41, 2443.
21. Chee, J. W.; Amirul, A. A.; Tengku Muhammad, T. S.; Majid, M. I. A.; Mansor, S. M. Biochem Eng J 2008, 38, 314.
22. Rahayu, A.; Zaleha, Z.; Yahya, A. R. M.; Majid, M. I. A.; Amirul, A. A. World J Microbiol Biotechnol 2008, 24, 2403.
23. Vigneswari, S.; Nik, L. A.; Majid, M. I. A.; Amirul, A. A. World J Microbiol Biotechnol 2010, 26, 743.
24. Faezah, A. N.; Rahayu, A.; Vigneswari, S.; Majid, M. I. A.; Amirul, A. A. World J Microbiol Biotecnol, to appear.
25. Mothes, G.; Ackermann, J. U. Eng Life Sci 2005, 5, 58.
26. Doi, Y. Microbial Polyesters; VCH: New York, 1990.
27. Chanprateep, S.; Kulpreecha, S. J Biosci Bioeng 2006, 101, 51.
28. Chai, H. L.; Rahayu, A.; Yahya, A. R. M.; Majid, M. I. A.; Amirul, A. A. Afr J Biotechnol 2009, 8, 4189.
29. Sudesh, K.; Abe, H.; Doi, Y. Prog Polym Sci 2000, 25, 1503.
30. Doi, Y.; Segawa, A.; Kunioka, M. Polym Commun 1989, 30, 169.
31. Nakamura, S.; Doi, Y.; Scandola, M. Macromolecules 1992, 25, 4237.
32. Hiramitsu, M.; Koyama, N.; Doi, Y. Biotechnol Lett 1993, 15, 461.
33. Saito, Y.; Doi, Y. Int J Biol Macromol 1994, 16, 99.
34. Kusaka, S.; Iwata, T.; Doi, Y. J Macromol Sci A 1998, 35, 319.
35. Tomasi, G.; Scandola, M.; Briese, B. H.; Jendrossek, D. Macromolecules 1996, 29, 507.
36. Riande, E.; Diaz-Calleja, R.; Prolongo, M. G.; Masegosa, R. M.; Salom, C. Polymer Viscoelasticity, Stress and Strain in Practice. Marcel Dekker Inc.: Basel, New York, 2000.
37. Liang, Y. S.; Zhao, W.; Chen, G. Q. J Biomed Mater Res A 2008, 87, 441.
38. Shi, G.; Cai, Q.; Wang, C.; Lu, N.; Wang, S.; Bei, J. Polym Adv Technol 2002, 13, 227.
39. Barbanti, S. H.; Santos, A. R.; Zavaglia, A. C.; Duel, A. R. J Mater Sci-Mater Med 2004, 15, 1315.
40. Hutmacher, D. W. Biomaterials 2000, 21, 2529.
41. Abe, H.; Doi, Y.; Kumagai, Y. Macromolecules 1994, 27, 6012.
42. Tomasi, G.; Scandola, M.; Briese, B. H.; Jendrossek, D. Macromolecules 1996, 29, 507.
43. Böstman, O.; Pihlajamäki, H. Biomaterials 2000, 21, 2615.
44. Anselme, K. Biomaterials 2000, 21, 667.